Journal of Microbiological Methods 201 (2022) 106578

Contents lists available at ScienceDirect

Journal of Microbiological Methods

journal homepage: www.elsevier.com/locate/jmicmeth

Naked-eye detection of *Staphylococcus aureus* in powdered milk and infant formula using gold nanoparticles

Marco Marin [a], Francesco Rizzotto [a], Vincent Léguillier [a], Christine Péchoux [b], Elise Borezee-Durant [a], Jasmina Vidic [a,*]

[a] Université Paris-Saclay, INRAE, AgroParisTech, Micalis Institute, 78350 Jouy-en-Josas, France
[b] Université Paris-Saclay, INRAE, GABI, 78350 Jouy-en-Josas, France

ARTICLE INFO

Keywords:
Gold nanoparticles
Food matrix effect
Aptamer
Colorimetric detection

ABSTRACT

Nonspecific binding of proteins from complex food matrices is a significant challenge associated with a biosensor using gold nanoparticles (AuNPs). To overcome this, we developed an efficient EDTA chelating treatment to denature milk proteins and prevent their adsorption on AuNPs. The use of EDTA to solubilize proteins enabled a sensitive label-free apta-sensor platform for colorimetric detection of *Staphylococcus aureus* in milk and infant formula. In the assay, *S. aureus* depleted aptamers from the test solution, and the reduction of aptamers enabled aggregation of AuNPs upon salt addition, a process characterized by a color change from red to purple. Under optimized conditions, *S. aureus* could be visually detected within 30 min with the detection limit of 7.5×10^4 CFU/mL and 8.4×10^4 CFU/mL in milk and infant formula, respectively. The EDTA treatment provides new opportunities for monitoring milk contamination and may prove valuable for biosensor point-of-need applications.

1. Introduction

Staphylococcus aureus, commonly called "golden staph", is a highly versatile human and animal pathogen and a major health concern due to accrued resistance to antibiotics. It is a Gram-positive opportunistic bacterium present on human skin and mucous in approximately 30% of the healthy population (Ryu et al., 2014). It is also frequently present in the air, dust, water and on environmental surfaces (Hennekinne et al., 2012). In humans and animals, *S. aureus* can cause different kinds of illnesses from minor skin infections to persistent intracellular infections and life-threatening septicemia. Additionally, it is the major cause of mastitis (Holmes and Zadoks, 2011; Kadariya et al., 2014) which leads to the hygienic standards inadequacy for the human consumption of milk derived from animals affected by this illness. Finally, *S. aureus* has high potential for milk poisoning since it can produce seven different toxins that are heat resistant and survive pasteurization (Rajkovic et al., 2020).

Milk and dairy products are considered vehicles of *S. aureus* for infection in humans. The contamination may arrive along the production chain, during storage and distribution when hygienic milking conditions are not fully respected, but also via contaminated milking equipment (Hennekinne et al., 2012; Rubab et al., 2018). Cross-contamination by *S. aureus* during handling have been reported for powdered infant formula as well (Cho et al., 2019), which poses a serious health risk to newborns that do not have fully developed immune system. Efficient detection of *S. aureus* is of pronounce importance to prevent bacterium spread, and reduce risks associated with public health and food safety.

The traditional methods used for *S. aureus* detection are culture-based. They include sample preparation, enrichment, colony selection and enumeration, and a confirmation test (Cossettini et al., 2022; Vidic et al., 2019; Vizzini et al., 2019). Although accurate and sensitive, traditional methods are very laborious and need several days to yield results (Kotsiri et al., 2022; Ramarao et al., 2020; Vidic et al., 2017). Molecular technologies, such as MALDI-TOF mass spectroscopy, polymerase chain reaction (PCR), next generation sequencing, or enzyme-

Abbreviations: AuNPs, gold nanoparticles; BHI, brain-heart-infusion; EDTA, ethylenediaminetetraacetic acid; ELISA, enzyme-linked immunosorbent assay; LSPR, localized surface plasmon resonance; MALDI-TOF, Matrix Assisted Laser Desorption Ionization - Time of Flight; PCR, polymerase chain reaction; PBS, phosphate buffered saline; TCA, trichloroacetic acid.

* Corresponding author.
E-mail address: jasmina.vidic@inrae.fr (J. Vidic).

https://doi.org/10.1016/j.mimet.2022.106578
Received 17 July 2022; Received in revised form 7 September 2022; Accepted 7 September 2022
Available online 13 September 2022

linked immunosorbent assay (ELISA), have also been developed (Kotsiri et al., 2022; Rubab et al., 2018). Although providing the result in several hours, molecular methods are not widely used because they require skilled staff and expensive laboratory facilities, and still frequently well-isolated colonies (Nouri et al., 2018; Vidic et al., 2019). Moreover, molecular methods may provide false negative results due to inhibitory activity of milk components on DNA polymerase and milk fat interferences in DNA extraction (Cossettini et al., 2022; Schrader et al., 2012; Vidic et al., 2020).

Over the last decade, nanotechnology has been increasing in relevance as an innovative tool for food safety assessment (Bobrinetskiy et al., 2021; Chen et al., 2018; Kumar et al., 2014). Different nanomaterial based assays have been develop to detect *S. aureus* including electrochemical (Eissa and Zourob, 2020; Vidic and Manzano, 2021; Xu et al., 2018), magnetic (Duarte et al., 2017; Martins et al., 2019), piezoelectric (Lian et al., 2015), and plasmonic (Abbaspour et al., 2015; Aura et al., 2017; Balbinot et al., 2021; Rüppel et al., 2018). Among plasmonic biosensors, those using gold nanoparticles (AuNPs) are particularly promising, because they can meet the international guidelines for diagnostics known as REASSURED (Real-time connectivity; Ease of specimen collection; Affordability; Sensitivity; Specificity; User-friendliness; Rapid & robust operation; Equipment-free; and Deliverability) (Land et al., 2019). AuNPs can be easily functionalized with biological molecules that ensure recognition (antibody, DNA), and allow a naked-eye detection of intact bacterial cells due to the Localized Surface Plasmon Resonance (LSPR) phenomenon (Marin et al., 2021). LSPR depends on the AuNPs refractive index that reflects nanoparticles size, morphology and inter-particle distance, as review recently (Marin et al., 2021). These parameters may be altered upon AuNPs aggregation or upon particles binding to bacterial cells, which induce a color change of the particle solution: the more the distance between AuNPs is reduced upon aggregation, the intensity of the change in color from red to purple is greater.

However, although colorimetric LSPR biosensors enable rapid and point-of-need pathogen detection they can hardly be directly applied in complex food because of the inhibitory matrix effect (Chen et al., 2018). It was shown that matrix proteins could cause the loss of detection signals up to 80% in apta-sensors, immuno-sensors and fluorescent biosensors based on AuNPs (Tao et al., 2020).

The aim of this study was to develop and optimize an aptamer-based LSPR assay for *S. aureus* detection in milk and infant formula by improving both technology and sample treatment. Aptamers are short single-stranded oligonucleotides (DNA or RNA) that both recognize and bind to specific targets similarly as antibodies and adsorb on AuNPs (Zhang and Liu, 2021). Milk products are among the most challenging food matrices for colorimetric tests because they contain components such as butterfat globules, carbohydrates, proteins, and various minerals (Quigley et al., 2013), that interact strongly with AuNPs and interfere with the assay result (Marin et al., 2021). By performing a single additional step prior to analysis to eliminate the matrix hindrance issue, a good LSPR sensor performance was demonstrated in both products. Our work demonstrates that the simple treatment opens the possibility for the rapid and naked-eye detection of *S. aureus* in milk products at the point-of-need.

2. Materials and methods

2.1. Chemicals and reagents

AuNPs (20 nm), ethylenediaminetetraacetic acid (EDTA), Triton X100, hydrochloric acid (HCl), trichloroacetic acid (TCA) and phosphate buffered saline (PBS) were purchased from Sigma-Aldrich (Saint Quentin Fallavier, France) in analytical grade. AuNPs (20 nm), were purchased from Thermo Fisher Scientific (Illkirch, France). Powdered milk (Laboratoires Novalac SA, Genève, Switzerland) and infant formula (Novalec1) were purchased in the local supermarket. Aptamers were obtained from Eurofins Genomics SAS (Nantes, France). The specific anti-*S. aureus* aptamer (Apt1) was previously selected (Abbaspour et al., 2015) and had the following sequence: 5'-TCC CTA CGG CGC TAA CCC CCC CAG TCC GTC CTC CCA GCC TCA CAC CGC CAC CGT GCT ACA AC-3′, while the control linear DNA (Campy) was 5′- GGG AGA GGC AGA TGG AAT TGG TGG TGT AGG GGT AAA ATC CGT AGA −3′. The stock solutions of the aptamers (100 μM) were prepared using miliQ water and kept at −20 °C until use.

Table 1
Bacterial strains used in this study.

Microorganisms	Collection code
Staphylococcus aureus	FPR3757 USA300 [A]
Escherichia coli K12	ATCC 14948 [B]
Salmonella enteritidis	405/2006[C]
Bacillus cereus	ATCC 14579 [B]
B. cereus S51	S51 [C]
Pseudomonas aeruginosa	ATCC 27853 [B]
Klebsiella pneumoniae	ATCC 700603 [B]
Bacillus cytotoxicus	NVH 391–98 [D]

Source/Reference: [A],(Schlag et al., 2007); [B], American Type Culture Collection (Manassas, VA, USA) [C], INRAE collection (Jouy en Josas, France); [D], (Lund et al., 2000).

2.2. Bacterial strains

All strains used in this study are listed in Table 1. Strains were grown in brain-heart-infusion (BHI) medium, Becton Dickinson (DB, Le Pont de Claix, France), with shaking at 37 °C or on BHI agar at 37 °C.

2.3. Milk treatments

Powdered milk or infant formula was solubilized with milliQ water to obtain 1% solution and inoculated with bacterial cells. Bacterial cells were collected carefully from an overnight culture by centrifugation at 3000 rpm for 5 min, at room temperature and washed twice in PBS. Inoculates (500 μL), containing different bacterial concentrations, were added to 25 mL of milk or infant formula samples in a 250 mL Erlenmeyer flask. Flasks were incubated with shaking (200 rpm) at 37 °C for at least 30 min before testing.

After incubation, 3 mL of each sample were treated with (i) a double volume of 15 mM EDTA (pH 8 or 12) to denature proteins, (ii) 1 M HCl until reaching pH 3 to solubilize proteins; (iii) 600 μL of 10% TCA to precipitate proteins; or (iv) a double volume of 15 mM EDTA, pH 8 with 1% Triton X100 to solubilize proteins and fats. Samples were incubated for 10 min, then centrifuged at 10,000 rpm × 15 min and pellets were resuspended in 1 mL PBS before being analyzed by the aptasensor.

To estimate bacterial survival, the drop plate method was performed in order to compare bacterial concentration in treated and untreated in milk/infant formula samples. The final numbers of bacteria were determined using a drop plate method. For this, the inoculated solution was serially diluted by placing 100 μL of the suspension into a dilution tube containing 900 μL of PBS. This tube was vortexed, and 100 μL was removed and placed into a second dilution tube containing 900 μL of PBS. This process was repeated six times. Then, 10 μL of each dilution was plated on BHI agar and incubated for 18 h at 37 °C under aerobic condition. Colony counts from triplicate plates were converted to colony forming units/mL (CFU/mL).

2.4. Imaging bacterial cells

Bacteria viability in treated milk samples was estimated using a LIVE/DEAD BacLight kit (ThermoFisher, Ilkrich, France) and an AxioObserver.Z1 Zeiss optical microscope equipped with a Zeiss AxioCam MRm digital camera. The ZEN software package was used to process the images.

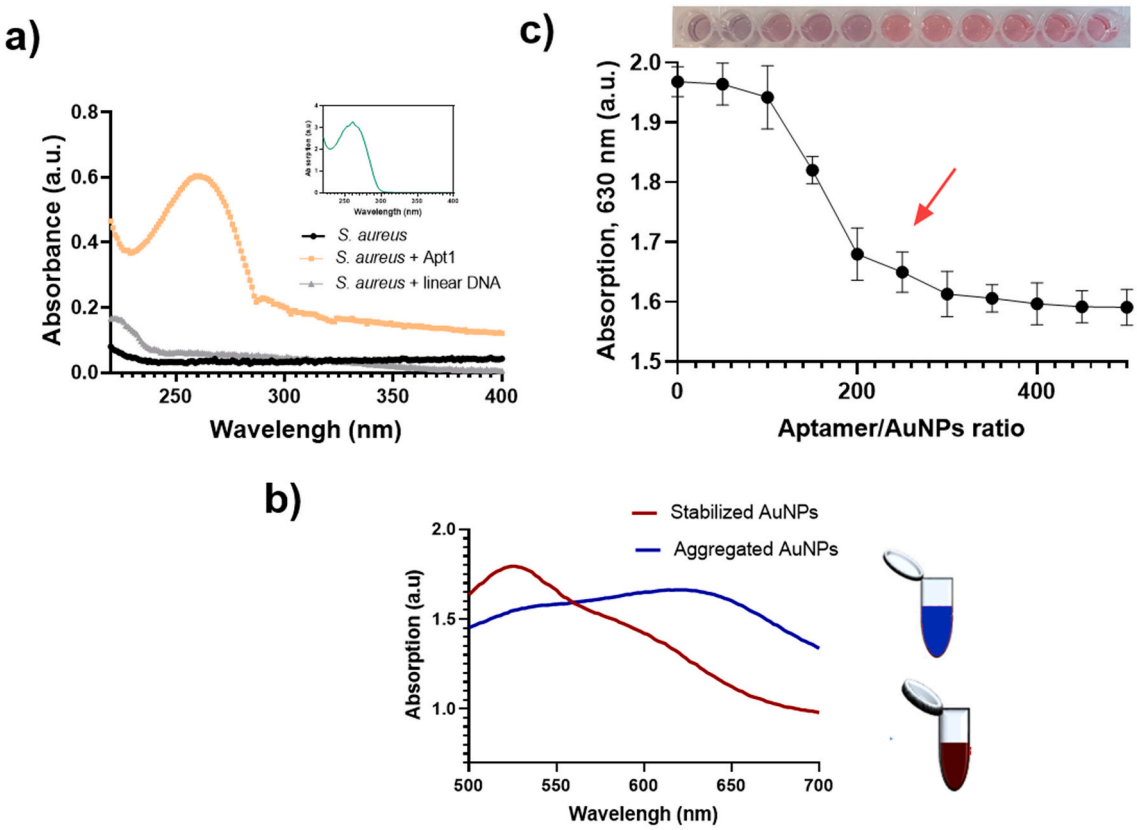

Fig. 1. (a) Spectrophotometric detection of Apt1 binding to *S. aureus* cells. The insert shows the adsorption spectra of Apt1. (b) Optimization of the molar ratio of Apt1 to AuNPs, mean ± SD of 3 measurements. The insert shows color changes of AuNPs solution at each ratio. (c) UV–Vis adsorption spectra of AuNPs before (stabilized AuNPs) and after $MgCl_2$ addition (aggregated AuNPs).

TEM analysis were performed to visualize interaction of *S. aureus* cells with AuNPs using a Hitachi HT7700 electron microscope operated at 80 kV (Elexience, France). Five µL of bacterial solution (10^6 CFU/mL) were added to 50 µL of AuNPs, and 5 µL PBS and incubated for 10 min. Then, 5 µL of 2 M $MgCl_2$ were added to aggregate nanoparticles. Two µl of the solution were collected onto 200-mesh copper grids, and visualized. Digital images were acquired using a charge-coupled device camera system (AMT).

2.5. Spectrophotometry

The specificity of Apt1 binding to *S. aureus* cells was evaluated using an UV–Vis spectrophotometer Biochrom Libra S22 (Biochrom Ltd., Cambridge, UK). Bacterial cells were washed and resuspended in 0.1 mM EDTA, 10 mM Tris-HCl, pH 8, to final concentration of 10^6 CFU/mL. *S. aureus* cells were incubated with 5 µM of Atp1 at 37 °C for 1 h in stirring conditions. Subsequently, bacterial cells were centrifuged at 3000 rpm × 5 min, the supernatant was removed and the pellet was resuspended in PBS for analysis. In control experiments, Apt1 was replaced by the linear DNA oligomer.

2.6. Aptasensor optimization

Optimization of the aptamer concentration was carried out using 50 µL of AuNPs solution (20 nm), 5 µL of PBS and 5 µL of different aptamer concentrations (ranging from 0 to 16.9 µM). After 10 min incubation under gentile shaking, 5 µL of 2 M $MgCl_2$ were added and the color change of the solutions was evaluated by measuring absorption at 520 nm and 630 nm (A630/A520) using Tecan plate reader (Tecan Infinite M200PRO, Männedorf, Switzerland).

2.7. Detection of S. aureus

Milk and infant formula were spiked with different concentrations of *S. aureus* (0 to 10^8 CFU/mL). Subsequently, 3 mL of each sample was treated with 6 mL of 15 mM EDTA, pH 8, centrifuged and resuspended in 1 mL PBS. Fifteen µL of resuspended bacterial cells was incubated with Apt1 (2 µM) for 10 min, then centrifuged at 3000 × rpm for 5 min. The supernatant containing unbound aptamer (5 µL) was incubated with 50 µL of AuNPs (0.27 pM). After equilibrating solutions at room temperature for 10 min, 5 µL of 2 M $MgCl_2$ were added, mixed, and incubated for another 15 min. Then, the solution was transferred to a 96-well plate for spectral recording using plate reader. All assays were performed at room temperature.

3. Results and discussion

3.1. Binding of Apt1 to S. aureus

Recognition of *S. aureus* cells by Apt1 was tested by UV–Vis spectroscopy. Apt1, as a DNA, has a maximum absorption at 260 nm (inset Fig. 1a). Bacterial cells (10^5 CFU/mL) in PBS showed no absorption peak at 260 nm (Fig. 1a). When cells were incubated with Apt1 and then thoroughly washed, a significant increase in the intensity of the peak at 260 nm was observed indicating the binding of Apt1 to *S. aureus*. Control tests performed with bacterial cells incubated with a linear oligonucleotide sequence did not produce peak intensity increase at 260 nm (Fig. 1a).

3.2. Optimization of Apt1 working concentration

Citrate capped AuNPs (20 nm) used here were electrically stabilized

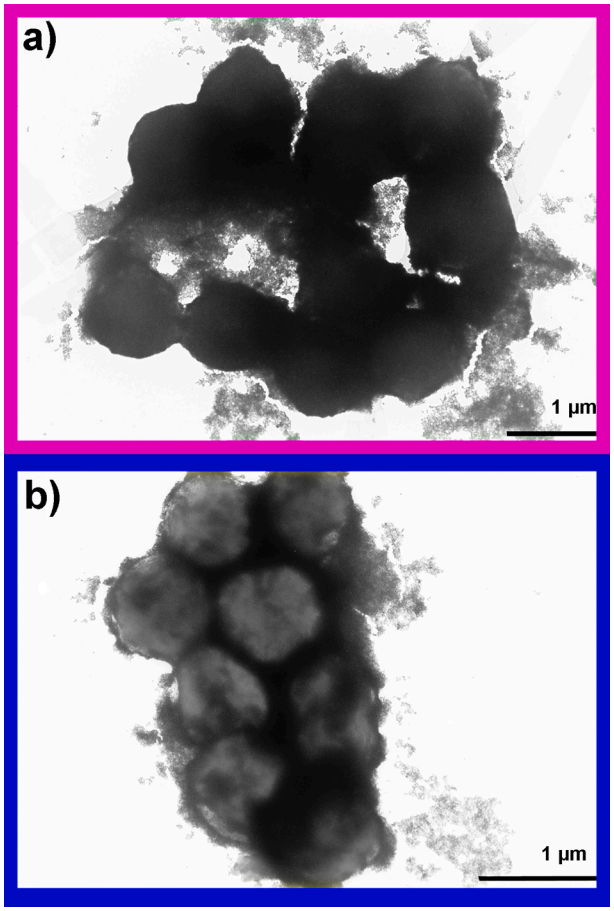

Fig. 2. Transmission electron micrographs of *S. aureus* cells and (a) unmodified AuNPs and (b) AuNPs carrying adsorbed Apt1. Note that in both cases bacterial cells/nanoparticle aggregates were formed.

and of a red color. By adding 5 μL of $MgCl_2$ of different concentrations to 50 μL of AuNPs, the color change of the solution was observed by naked eyes when final concentrations of $MgCl_2$ were higher than 200 mM. In several minutes, at such high ionic strengths, the solution changed from red (plasmonic band was at ~520 nm) to a blue-to-violet color (plasmonic band was at ~630 nm) due to nanoparticle aggregation (Fig. 1b). The aptamer adsorption on AuNPs may protect nanoparticles from salt-induced aggregation (Marin et al., 2021). The working concentration of Apt1 was optimized to control the stability of AuNPs by increasing the Apt1/AuNPs molar ratio (Fig. 1c). AuNPs rested stabilized at a molar ratio above 150:1 after addition of $MgCl_2$. At these high ratios, Apt1 molecules adsorbed on AuNPs and prevented aggregation. The protection was weak for lower the Apt1/AuNPs ratios and solutions of AuNPs changed to a violet color upon salt addition (Fig. 1c). Therefore, the ratio 150:1 (0.1 μM Apt1 final concentration) and 200 mM $MgCl_2$ were chosen for the aptasensor construction. The reaction time of 15 min was sufficient to observe the color change, and was further used in experiments.

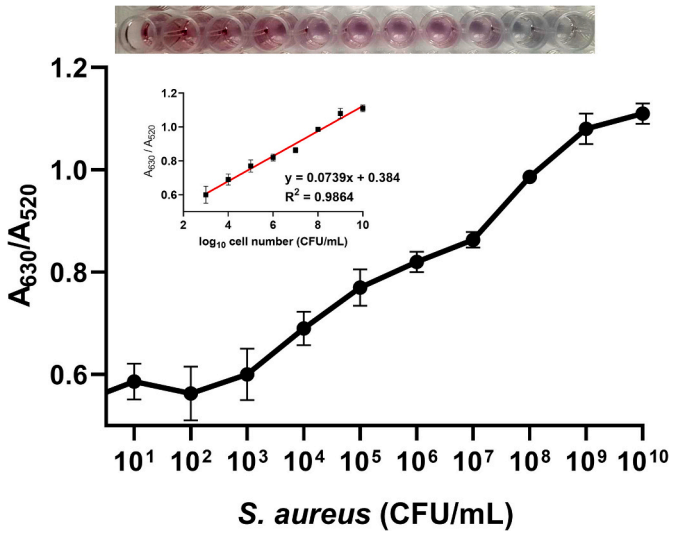

Fig. 3. Photographed image and colorimetric detection of *S. aureus* in PBS. The calibration curve of adsorption ratio 630/520 nm versus concentration of *S. aureus*. Insert graph show the derived calibration curve for corresponding means ± SD of 3 experiments. Insert photograph shows color changes of AuNPs at each concentration.

3.3. Development of the assay for S. aureus detection

Most reported aptasensors based on AuNPs work in a direct target-mediated AuNPs aggregation mode (Marin et al., 2021). However, when we applied it to detection of *S. aureus*, this approach led to a detection failure because nanoparticles adsorbed and aggregated on bacterial cells regardless their functionalization, as shown in Fig. 2.

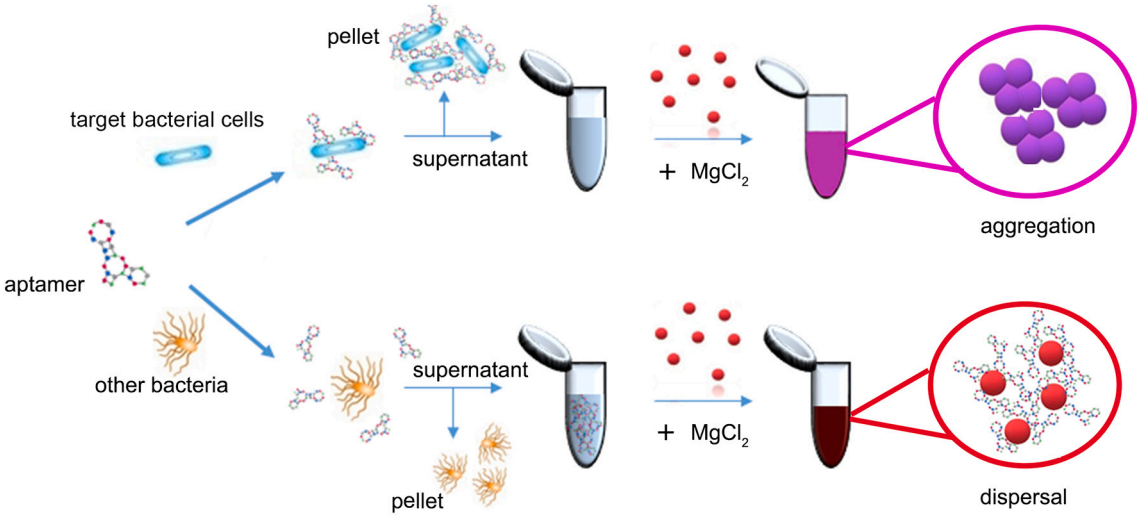

Schema 1. Graphical illustration of the designed two-stage detection of *S. aureus* using a colorimetric apta-sensor.

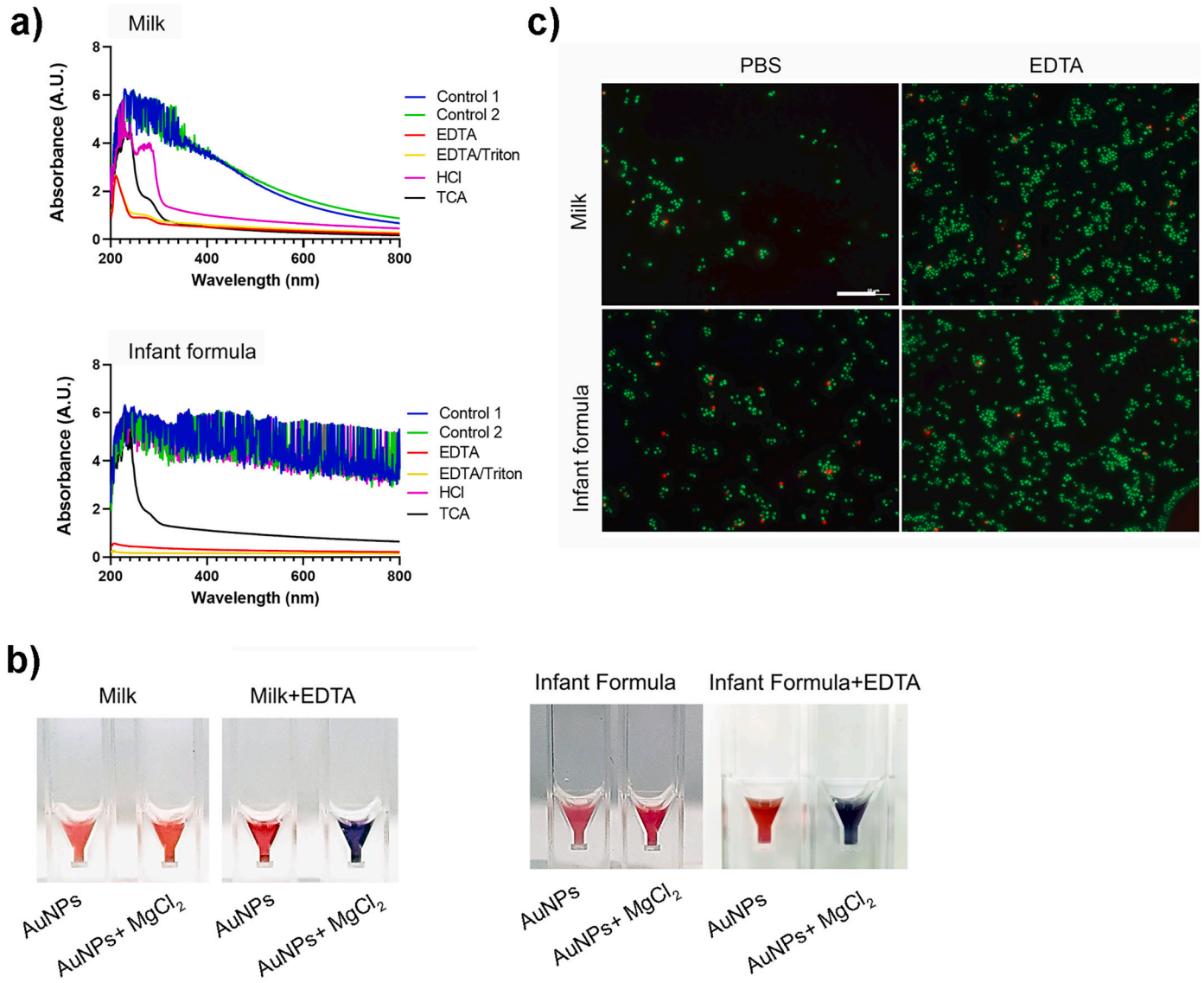

Fig. 4. (a) UV–Vis spectra of powder milk and infant formula water solutions before (Control1), and after inoculation with 10^5 CFU/mL *B. cerus* bacterial cells (Control2), and UV–Vis spectra of corresponding bacterial solutions treated with 15 mM EDTA (pH 8), 15 mM EDTA/ 1% Triton X-100, HCl (pH 3) and 2% TCA. (b) Effect of EDTA treatment to visualization of the salt addition to AuNPs admixed to noncontaminated milk and infant formula solutions. (c) LIVE/DEAD BacLight stain of *S. aureus* cells in milk and infant formula treated with 15 mM EDTA, pH 8. Scale bar, 5 μm stains for all images.

Despite the fact that both AuNPs and bacterial cells are of a negative surface charge, AuNPs seemed to bind bacterial cells by a nonspecific adsorption and aggregate. This phenomenon was not influenced by the absence and presence of Apt1 (Fig. 2). Moreover, the aggregation of non-functionalized AuNPs was observed with another milk contaminating bacterium *B. cereus* (Fig. S-1), suggesting that AuNPs may adsorb on other Gram-positive bacteria.

To eliminate the nonspecific binding between bacterial cells and AuNPs, an indirect assay was performed as illustrated in Schema 1. In the first step Apt1 was added to the sample and incubated for 10 min. In the absence of *S. aureus*, Apt1 diffused freely in the sample and could not be removed by centrifugation. In the second step, supernatants were added to AuNPs solution and aptamers prevented salt-induced aggregation. In contaminated samples Apt1 precipitated with bacterial cells enabling AuNPs to aggregate upon salt addition. The color change thus occurred only for positive samples and could be observed visually or measured by a spectrophotometer and expressed by the A_{630}/A_{520} ratio.

We evaluated the performance of the colorimetric two-step aptasensor for the detection of *S. aureus* in pure culture. Prior to detection bacterial cells, cultivated in BHI medium, were washed and resuspended in PBS. Fig. 3 shows that as the concentration of bacterial cells increased, the absorbance ratio (A_{630}/A_{520}) gradually increased. The proposed two-step detection mode was highly sensitive: a visible color change of AuNPs from red to blue due to aggregation can be seen in inset Fig. 3. The limit of detection was 10^3 CFU/mL visually, and 1 CFU/mL by UV–vis Spectrum (obtained by the eq. 3S/N, where S is the standard deviation of the blank solution, and N is the slope of the calibration curve, inset in Fig. 3). In addition, the dynamic range with a good linear response was obtained for *S. aureus* concentrations between 10^2 CFU/mL and 10^8 CFU/mL.

However, when this two-step assay was performed in inoculated milk and infant formula, the reactive solution color change was observed only for *S. aureus* at concentrations $\geq 10^8$ CFU/mL. Milk components strongly interfered with the apta-sensor. Probably, bacterial cells absorbed many milk components that desorbed during the test and prevent AuNPs aggregation. To adapt the test to complex milk-based products and increase the test sensitivity we next sought to eliminate the inhibitory matrix effect.

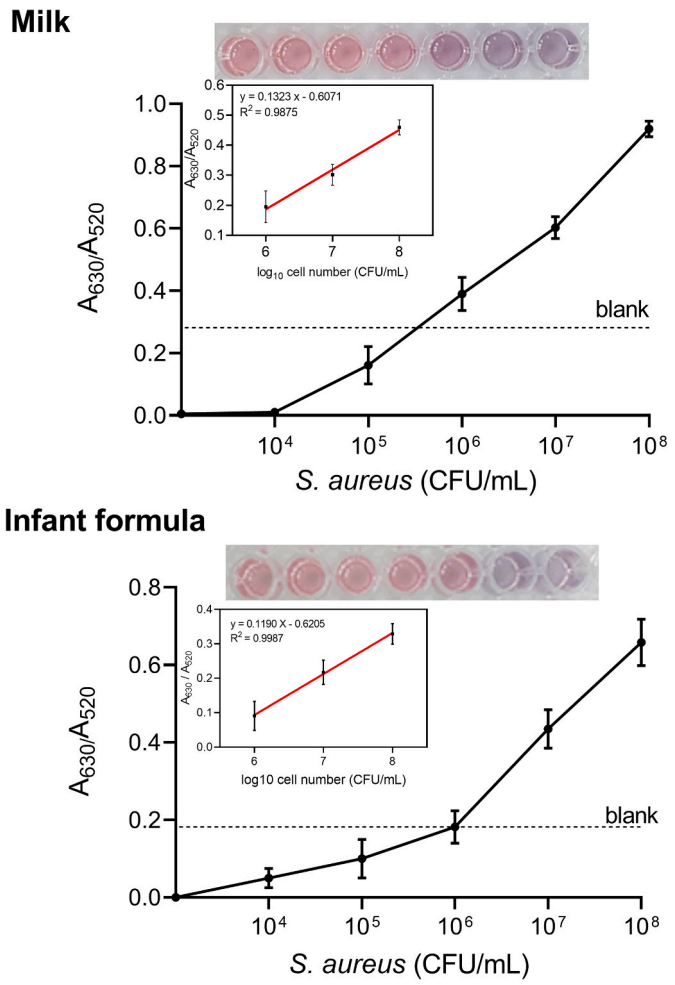

Fig. 5. Adsorption ratio at 630 and 520 nm of AuNPs versus concentration of *S. aureus* in inoculated milk and infant formula solutions. Insert graphs show the derived calibration curves for corresponding, means ± SD of 3 experiments. Insert photograph shows color changes of AuNPs at each concentration, where far-left and far-right wells correspond to negative control (2 μM Apt1) and positive control (no Apt1), respectively.

3.4. Milk and infant formula treatment

In the aim to make the test as simple and cheap as possible, we compared different treatments that eliminate proteins in milk and allow AuNPs aggregation upon salt addition. The UV–Vis spectroscopy of milk and infant formula showed that both food matrices strongly adsorb in the visible wavelength region confirming that direct spectroscopic observation of AuNPs aggregation would not be possible (Fig. 4a). Since Apt1 recognizes live bacterial cells the ideal treatment should eliminate the matrix effect without damaging bacterial cells. >80% of total milk proteins are caseins that together with a high proportion of calcium and phosphates are incorporated into lipidic micelles (Marathe et al., 2012). These proteins were denatured by addition of 2% TCA, HCl to reach pH 3, or by using chelating agent EDTA alone or in combination with Triton-X100 to solubilize micelles (Fig. 4a and Fig. S-2). All tests were performed in samples containing *Bacillus cereus* cells. *B. cereus* of a characteristic rod-shape and size of a few microns was chosen for easy optical microscope observation. The TCA treatment was not adapted for direct LSPR assays because of TCA precipitated proteins that were pelleted together with bacterial cells. The HCl treatment efficiently denatured proteins and made the solution transparent but damaged bacterial cells. Finally, EDTA caused protein unfolding and denaturing by sequestering calcium ions and disturbing micelles without injuring bacterial cells. By adding a double volume of 15 mM EDTA solution, solutions became transparent due to the milk protein unfolding (Makhzami et al., 2008), as illustrated in Fig. 4a. Interestingly, despite the fact that the infant formula sample was still of a white color (Fig. S-2) both EDTA-treated milk and infant formula showed no absorption in the visible region as presented in Fig. 4a. Similar efficiency to make the sample transparent was observed with the EDTA/Triton-X100 treatment (Fig. 4a). Triton-X100 was added to disperse fat flocculants containing proteins. For test simplicity, the EDTA treatment was chosen in further detection assays. Fig. 4b shows that EDTA addition to milk and infant formula containing AuNPs enabled naked-eye visualization of AuNPs aggregation upon salt addition. In contrast, no nanoparticle aggregation was observed in untreated samples.

To verify the non-toxicity of the EDTA treatment, analysis of the cytotoxic effects of the 15 mM EDTA on *S. aureus* was performed by enumeration of survival bacterial cells, and using the LIVE/DEAD BacLight Kit in combination with epifluorescence microscopy. No decrease in the bacterial cell number was obtained in EDTA-treated milk and infant formula inoculated with 10^5 CFU/mL *S. aureus* compared to the corresponding untreated samples. After staining of *S. aureus* cells with a SYBR Green I and PI mixture, living bacterial cells were of green fluorescence, and dead cells of red fluorescence. Fig. 4c clearly shows that most round-shaped *S. aureus* cells were alive in samples containing EDTA. The non-toxicity of 15 mM EDTA was confirmed using *B. cereus* cells in milk and infant formula samples (Fig. S-3).

3.5. Analytical performance of the apta-sensor in complex matrices

Utilizing the optimized conditions, the LSPR apta-sensor shows a linear response to *S. aureus* over a dynamic range of 10^4–10^8 CFU/mL cells in milk and infant formula (Fig. 5). The theoretical limit of detection was 7.5×10^4 CFU/mL and 8.4×10^4 CFU/mL of *S. aureus* in milk and infant formula, respectively. The visual limit of detection was 10^6 CFU/mL of *S. aureus* (insets Fig. 5). Despite the fact that such detection performances are inferior to some recently reported for other aptamer-based biosensors (Abbaspour et al., 2015; Tao et al., 2021), this colorimetric biosensor has advantages to be instrument free and performed in complex food matrices. Moreover, in contrast to colorimetric sensors coupled to signal amplification, our two-step assay is not connected to instrumentations which often require complex biochip-processing technology or expensive filters and set-ups.

The selectivity of the colorimetric apta-sensor for *S. aureus* was tested by comparing the obtained color change with that of other interfering bacteria under the same conditions. The results in Fig. 6 show that only solution of milk and infant formula spiked with *S. aureus* had a violet color, and their absorption variation (A_{630}/A_{520}) was significantly higher than that obtained with non-relating bacteria. This finding suggests that Apt1 did not bind to control strains and, thus, Apt1 in supernatants could adsorb to AuNPs and prevented their aggregation.

4. Conclusion

In summary, we developed a milk and infant formula treatment to increase the sensitivity of a direct colorimetric detection of *S. aureus* using an apta-sensor based on LSPR and AuNPs. In the assay, contaminated samples were evidenced through AuNPs aggregation and solution color change that could be compromised by matrix proteins. Specifically, our study suggested that milk proteins even in traces may adsorb on gold nanoparticles and significantly decrease the assay sensitivity. The addition of EDTA solubilized milk and infant formula macromolecules, which boosted the sensitivity of *S. aureus* detection. The obtained limit of detection suggests that the apta-sensor is suitable for screening dairy samples for *S. aureus* since its ingested infectious doses were reported to be over 10^{10} cells (Jankie et al., 2016).

The EDTA treatment made the assay a promising alternative for the design of novel biosensors. In case of detection of other milk

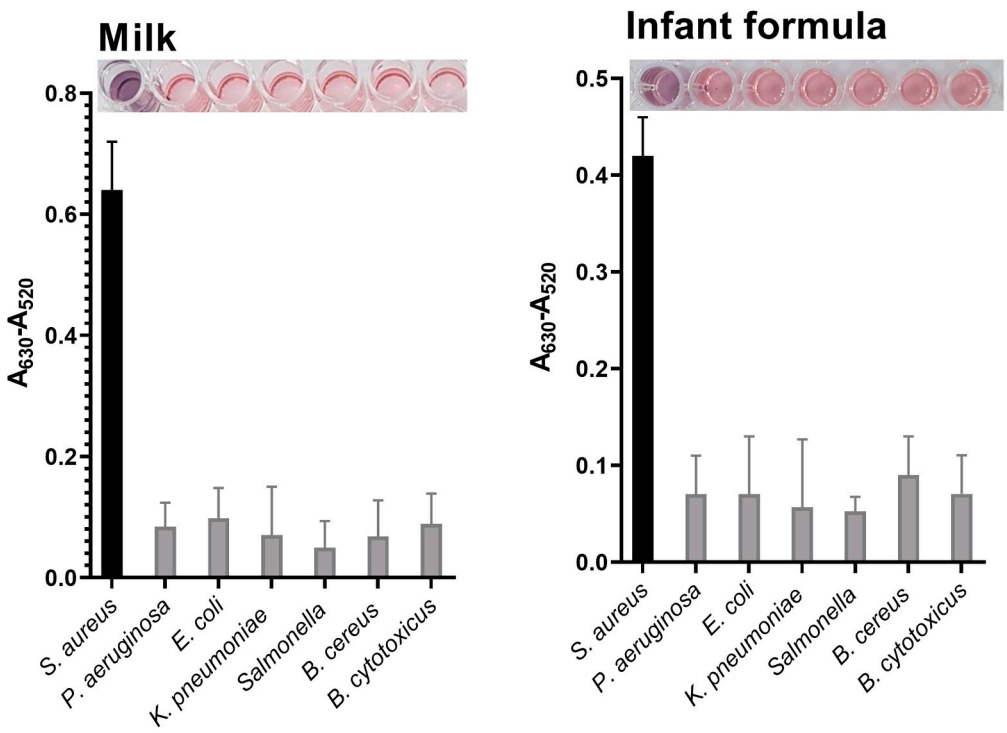

Fig. 6. Visual color and the adsorption ratio at 630 and 520 nm of the sensing solutions for *S. aureus* (10^6 CFU/mL) and six interfering bacteria (10^7 CFU/mL), mean ± SD of 3 experiments.

contaminating bacterial pathogens, such as *Campylobacter* or *Escherichia coli*, that have very low infectious doses (500 cells and 100 cells, respectively), the sensibility of the assay can be further improve by coupling AuNPs to an enzymatic reaction (Marin et al., 2021; Yuan et al., 2014) or other nanoparticles.

Supplementary data to this article can be found online at https://doi.org/10.1016/j.mimet.2022.106578.

Funding

This work is in a part supported by the French agency for research (ANR) for funding (Siena, ANR-21-CE21-0009-03), the DIM One-Health2021 and the European Union's Horizon 2020 research and innovation programme under the Marie Skłodowska–Curie grant agreement N° 872662 (IPANEMA).

Author contribution

M.M. Conceptualization, investigation, writing; F.R. formal analysis, investigation, writing original draft. V.L. formal analysis; C.P. formal analysis, E.BD. methodology, editing, and J.V. conceptualization, investigation, funding aquisition, project administration, supervision, writing original draft, editing. All authors approved the final version of the article.

Declaration of Competing Interest

The authors declare that they have no known competing financial interests or personal relationships that could have appeared to influence the work reported in this paper.

Data availability

No data was used for the research described in the article.

Acknowledgments

We acknowledge the MIMA2 platform for access to electron microscopy equipment (MIMA2, INRAE, 2018. Microscopy and Imaging Facility for Microbes, Animals and Foods, https://doi.org/10.15454/1.5572348210007727E12), Thierry Meylheuc (INRAE, France) for his expertise with scanning electron microscopy, Mayura Subramaniam (Université Paris-Sacaly, France) for technical assistance and Maria Vesna Nikolic (University of Belgrade, Serbia) for discussion and critical reading of the manuscript.

References

Abbaspour, A., Norouz-Sarvestani, F., Noori, A., Soltani, N., 2015. Aptamer-conjugated silver nanoparticles for electrochemical dual-aptamer-based sandwich detection of *Staphylococcus aureus*. Biosens. Bioelectron. 68, 149–155.

Aura, A.M., D'Agata, R., Spoto, G., 2017. Ultrasensitive detection of *Staphylococcus aureus* and *Listeria monocytogenes* genomic DNA by nanoparticle-enhanced surface Plasmon resonance imaging. Chemistryselect 2 (24), 7024–7030.

Balbinot, S., Srivastav, A.M., Vidic, J., Abdulhalim, I., Manzano, M., 2021. Plasmonic biosensors for food control. Trends Food Sci. Technol. 111, 128–140.

Bobrinetskiy, I., Radovic, M., Rizzotto, F., Vizzini, P., Jaric, S., Pavlovic, Z., Radonic, V., Nikolic, M.V., Vidic, J., 2021. Advances in nanomaterials-based electrochemical biosensors for foodborne pathogen detection. Nanomaterials 11 (10), 2700.

Chen, H., Zhou, K., Zhao, G., 2018. Gold nanoparticles: from synthesis, properties to their potential application as colorimetric sensors in food safety screening. Trends Food Sci. Technol. 78, 83–94.

Cho, T.J., Hwang, J.Y., Kim, H.W., Kim, Y.K., Kwon, J.I., Kim, Y.J., Lee, K.W., Kim, S.A., Rhee, M.S., 2019. Underestimated risks of infantile infectious disease from the caregiver's typical handling practices of infant formula. Sci. Rep. 9 (1), 1–12.

Cossettini, A., Vidic, J., Maifreni, M., Marino, M., Pinamonti, D., Manzano, M., 2022. Rapid detection of *Listeria monocytogenes*, Salmonella, *Campylobacter* spp., and *Escherichia coli* in food using biosensors. Food Control 108962.

Duarte, C.M., Carneiro, C., Cardoso, S., Freitas, P.P., Bexiga, R., 2017. Semi-quantitative method for Staphylococci magnetic detection in raw milk. J. Dairy Res. 84 (1), 80.

Eissa, S., Zourob, M., 2020. Ultrasensitive peptide-based multiplexed electrochemical biosensor for the simultaneous detection of *Listeria monocytogenes* and *Staphylococcus aureus*. Microchim. Acta 187 (9), 1–11.

Hennekinne, J.-A., De Buyser, M.-L., Dragacci, S., 2012. Staphylococcus aureus and its food poisoning toxins: characterization and outbreak investigation. FEMS Microbiol. Rev. 36 (4), 815–836.

Holmes, M.A., Zadoks, R.N., 2011. Methicillin resistant *S. aureus* in human and bovine mastitis. J. Mammary Gland Biol. Neoplasia 16 (4), 373–382.

Jankie, S., Jenelle, J., Suepaul, R., Pereira, L.P., Akpaka, P., Adebayo, A.S., Pillai, G., 2016. Determination of the infective dose of *Staphylococcus aureus* (ATCC 29213) and *Pseudomonas aeruginosa* (ATCC 27853) when injected intraperitoneally in Sprague Dawley rats. J. Pharm. Res. Int. 1–11.

Kadariya, J., Smith, T.C., Thapaliya, D., 2014. *Staphylococcus aureus* and staphylococcal food-borne disease: an ongoing challenge in public health. Biomed. Res. Int. 2014.

Kotsiri, Z., Vidic, J., Vantarakis, A., 2022. Applications of biosensors for bacteria and virus detection in food and water–a systematic review. J. Environ. Sci. 111, 367–379.

Kumar, N., Seth, R., Kumar, H., 2014. Colorimetric detection of melamine in milk by citrate-stabilized gold nanoparticles. Anal. Biochem. 456, 43–49.

Land, K.J., Boeras, D.I., Chen, X.-S., Ramsay, A.R., Peeling, R.W., 2019. REASSURED diagnostics to inform disease control strategies, strengthen health systems and improve patient outcomes. Nat. Microbiol. 4 (1), 46–54.

Lian, Y., He, F., Wang, H., Tong, F., 2015. A new aptamer/graphene interdigitated gold electrode piezoelectric sensor for rapid and specific detection of *Staphylococcus aureus*. Biosens. Bioelectron. 65, 314–319.

Lund, T., De Buyser, M.L., Granum, P.E., 2000. A new cytotoxin from *Bacillus cereus* that may cause necrotic enteritis. Mol. Microbiol. 38 (2), 254–261.

Makhzami, S., Quénée, P., Akary, E., Bach, C., Aigle, M., Delacroix-Buchet, A., Ogier, J.-C., Serror, P., 2008. In situ gene expression in cheese matrices: application to a set of enterococcal genes. J. Microbiol. Methods 75 (3), 485–490.

Marathe, S.A., Chowdhury, R., Bhattacharya, R., Nagarajan, A.G., Chakravortty, D., 2012. Direct detection of *Salmonella* without pre-enrichment in milk, ice-cream and fruit juice by PCR against hilA gene. Food Control 23 (2), 559–563.

Marin, M., Nikolic, M.V., Vidic, J., 2021. Rapid point-of-need detection of bacteria and their toxins in food using gold nanoparticles. Compr. Rev. Food Sci. Food Saf. 20 (6), 5880–5900.

Martins, S.A., Martins, V.C., Cardoso, F.A., Germano, J., Rodrigues, M., Duarte, C., Bexiga, R., Cardoso, S., Freitas, P.P., 2019. Biosensors for on-farm diagnosis of mastitis. Front. Bioeng. Biotechnol. 7, 186.

Nouri, A., Ahari, H., Shahbazzadeh, D., 2018. Designing a direct ELISA kit for the detection of *Staphylococcus aureus* enterotoxin a in raw milk samples. Int. J. Biol. Macromol. 107, 1732–1737.

Quigley, L., O'Sullivan, O., Stanton, C., Beresford, T.P., Ross, R.P., Fitzgerald, G.F., Cotter, P.D., 2013. The complex microbiota of raw milk. FEMS Microbiol. Rev. 37 (5), 664–698.

Rajkovic, A., Jovanovic, J., Monteiro, S., Decleer, M., Andjelkovic, M., Foubert, A., Beloglazova, N., Tsilla, V., Sas, B., Madder, A., 2020. Detection of toxins involved in foodborne diseases caused by gram-positive bacteria. Compr. Rev. Food Sci. Food Saf. 19 (4), 1605–1657.

Ramarao, N., Tran, S.-L., Marin, M., Vidic, J., 2020. Advanced methods for detection of *Bacillus cereus* and its pathogenic factors. Sensors 20 (9), 2667.

Rubab, M., Shahbaz, H.M., Olaimat, A.N., Oh, D.-H., 2018. Biosensors for rapid and sensitive detection of *Staphylococcus aureus* in food. Biosens. Bioelectron. 105, 49–57.

Rüppel, N., Tröger, V., Sandetskaya, N., Kuhlmeier, D., Schmieder, S., Sonntag, F., 2018. Detection and identification of *Staphylococcus aureus* using magnetic particle enhanced surface plasmon spectroscopy. Eng. Life Sci. 18 (4), 263–268.

Ryu, S., Song, P.I., Seo, C.H., Cheong, H., Park, Y., 2014. Colonization and infection of the skin by *S. aureus*: immune system evasion and the response to cationic antimicrobial peptides. Int. J. Mol. Sci. 15 (5), 8753–8772.

Schlag, S., Nerz, C., Birkenstock, T.A., Altenberend, F., Götz, F., 2007. Inhibition of staphylococcal biofilm formation by nitrite. J. Bacteriol. 189 (21), 7911–7919.

Schrader, C., Schielke, A., Ellerbroek, L., Johne, R., 2012. PCR inhibitors–occurrence, properties and removal. J. Appl. Microbiol. 113 (5), 1014–1026.

Tao, X., Chang, X., Wan, X., Guo, Y., Zhang, Y., Liao, Z., Song, Y., Song, E., 2020. Impact of protein corona on noncovalent molecule–gold nanoparticle-based sensing. Anal. Chem. 92 (22), 14990–14998.

Tao, X., Liao, Z., Zhang, Y., Fu, F., Hao, M., Song, Y., Song, E., 2021. Aptamer-quantum dots and teicoplanin-gold nanoparticles constructed FRET sensor for sensitive detection of *Staphylococcus aureus*. Chin. Chem. Lett. 32 (2), 791–795.

Vidic, J., Manzano, M., 2021. Electrochemical biosensors for rapid pathogen detection. Curr. Opin. Electrochem. 100750.

Vidic, J., Manzano, M., Chang, C.-M., Jaffrezic-Renault, N., 2017. Advanced biosensors for detection of pathogens related to livestock and poultry. Vet. Res. 48 (1), 1–22.

Vidic, J., Vizzini, P., Manzano, M., Kavanaugh, D., Ramarao, N., Zivkovic, M., Radonic, V., Knezevic, N., Giouroudi, I., Gadjanski, I., 2019. Point-of-need DNA testing for detection of foodborne pathogenic bacteria. Sensors 19 (5), 1100.

Vidic, J., Chaix, C., Manzano, M., Heyndrickx, M., 2020. Food sensing: detection of *Bacillus cereus* spores in dairy products. Biosensors 10 (3), 15.

Vizzini, P., Braidot, M., Vidic, J., Manzano, M., 2019. Electrochemical and optical biosensors for the detection of *Campylobacter* and *Listeria*: an update look. Micromachines 10 (8), 500.

Xu, L., Liang, W., Wen, Y., Wang, L., Yang, X., Ren, S., Jia, N., Zuo, X., Liu, G., 2018. An ultrasensitive electrochemical biosensor for the detection of mecA gene in methicillin-resistant *Staphylococcus aureus*. Biosens. Bioelectron. 99, 424–430.

Yuan, J., Wu, S., Duan, N., Ma, X., Xia, Y., Chen, J., Ding, Z., Wang, Z., 2014. A sensitive gold nanoparticle-based colorimetric aptasensor for *Staphylococcus aureus*. Talanta 127, 163–168.

Zhang, F., Liu, J., 2021. Label-free colorimetric biosensors based on aptamers and gold nanoparticles: a critical review. Anal. Sens. 1 (1), 30–43.